

# JOURNAL OF THE AMERICAN CHEMICAL SOCIETY

© Copyright 1987 by the American Chemical Society

VOLUME 109, NUMBER 2

JANUARY 21, 1987

## Kinetic and Theoretical Study on the Ion/Molecule Reactions of Methoxymethyl Cation with Ammonia

Satoshi Okada,\*<sup>1a</sup> Yasuo Abe,<sup>1a</sup> Setsuo Taniguchi,<sup>1a</sup> and Shinichi Yamabe\*<sup>1b</sup>

Contribution from the Radiation Center of Osaka Prefecture, Shinke-cho, Sakai 593, Japan, and the Educational Technology Center, Nara University of Education, Takabatake-cho, Nara 630, Japan. Received July 28, 1986

**Abstract:** The reaction between  $C_2H_5O^+$  and  $NH_3$  is investigated by using the ion-trapping technique. Rate constants of reactions 3, 4, and 5 are determined. Their potential energy profiles are sought by use of the ab initio MO calculation. Reaction 3 gives the products methanol and protonated methylenimine. It is composed of the nucleophilic addition of  $NH_3$  to the carbonyl carbon and the subsequent 1,3-proton shift. Reaction 4 gives formaldehyde and protonated methylamine. It is of the  $S_N2$  type. Reaction 5 gives ammonium ion and ethylene oxide. The last reaction is of the specific pattern in the gas phase, although the reverse reaction involves the popular mechanism of the electrophilic ring cleavage.

Ion/molecule reactions in the gas phase have an important role to elucidate the mechanism of organic chemistry. It is an attractive subject to study whether the solvent-free reaction has the same pattern as that in the condensed phase or not. It is a goal to separate the intrinsic reactivity of the substrate from the solvent effect.

The reaction of the methoxymethyl cation  $CH_3OCH_2^+$  with a base is known to give several products.<sup>2-7</sup> However, it is not yet solved what kind of process is involved. In this work, kinetics of the reaction between methoxymethyl cation and ammonia are studied by using the ion-trapping technique.<sup>8-11</sup> To investigate the reaction process, an ab initio MO calculation is also made. The aim of this work is to judge whether reactions of  $CH_3OCH_2^+$  with  $NH_3$  involve the established mechanism of organic chemistry or the specific pattern in the gas phase.

### Experimental Section

The reactions have been studied by using the technique for ion trapping in the ion source of a mass spectrometer described by Bourne and Danby.<sup>8</sup> This technique has been used to study the ion/molecule reac-

**Table I.** Rate Constants for the Reactions of  $CH_3O^+$  with  $CH_3OCH_3$  and  $NH_3$

reaction	$10^{-10}k$ , $cm^3/(molecule \cdot s)$	
	this work (433 K)	other works
(1) $CH_3O^{+a} + CH_3OCH_3 \xrightarrow{k_1} CH_3OCH_2^+ + CH_3OH$	$9.6 \pm 1$	$11.6 \pm 1.5^b$
(2) $CH_3O^+ + NH_3 \xrightarrow{k_2} NH_4^+ + CH_2O$	$8 \pm 1$	$8.57^c$

<sup>a</sup> $m/z$  31. <sup>b</sup>Reference 2. <sup>c</sup>Reference 5.

tions by Harrison<sup>9,10</sup> and Ryan.<sup>11</sup> Ions were produced during the short pulse (1  $\mu s$ ) of an ionizing electron of suitable energy (15–25 eV). The ions were trapped in the negative space charge created by an electron beam whose energy is insufficient to cause ionization. The ions trapped were left to react successively further. A small negative bias was applied to repeller plates to obtain efficient ion trapping. The ions were removed for the mass analysis by applying a positive pulse of 2- $\mu s$  duration and 10-V amplitude to the repeller plates. Ion currents were detected by a 16-stage electron multiplier as a function of delay time (up to 1.8 ms) between the ionizing pulse and the ion removal pulse.

Source concentrations of the reaction gases were not measured directly but were related to the concentration in the inlet system from measurements of the disappearance rate of the  $CH_4^+$  in pure methane. A rate constant of  $1.1 \times 10^{-9} cm^3/(molecule \cdot s)$  for the reaction<sup>12</sup>  $CH_4^+ + CH_4 \rightarrow CH_5^+ + CH_3$  was used. All experiments were carried out at an ion source temperature, 433 K.

The ammonia and methane used were of Takachiho Research grade. Dimethyl ether and ammonia- $d_3$  solution were from Wako Pure Chemicals and purified by vacuum distillation before use. Mass spectrometric analysis of ammonia- $d_3$  gas revealed 90%  $ND_3$  and 10%  $ND_2H$ .

Figure 1 shows the semilogarithmic plots of normalized ion intensities of major ions observed in the  $CH_3OCH_3-NH_3$  system. The reactant ion was mainly  $C_2H_5O^+$ . The initial increase of the  $C_2H_5O^+$  ion at less than

(1) (a) Radiation Center of Osaka Prefecture. (b) Nara University of Education.

(2) Blair, A. S.; Harrison, A. G. *Can. J. Chem.* **1973**, *51*, 703.

(3) Van Doorn, R.; Nibbering, N. M. M. *Org. Mass Spectrom.* **1978**, *13*, 527.

(4) Pau, J. K.; Kim, J. K.; Caserio, M. C. *J. Am. Chem. Soc.* **1978**, *100*, 3838.

(5) Matsumoto, A.; Okada, S.; Taniguchi, S.; Hayakawa, T. *Bull. Chem. Soc. Jpn.* **1975**, *48*, 3387.

(6) Caserio, M. C.; Kim, J. K. *J. Org. Chem.* **1982**, *47*, 2940.

(7) Kinter, M. T.; Bursey, M. M. *J. Am. Chem. Soc.* **1986**, *108*, 1797.

(8) Bourne, A. J.; Danby, C. J. *J. Sci. Instrum.* **1968**, 155.

(9) Herod, A. A.; Harrison, A. G. *Int. J. Mass Spectrom. Ion Phys.* **1970**, *4*, 415.

(10) Harrison, A. G.; Lin, P. H.; Tsang, C. W. *Int. J. Mass Spectrom. Ion Phys.* **1976**, *19*, 23.

(11) Ryan, K. R.; Graham, I. G. *J. Chem. Phys.* **1973**, *59*, 4260.

(12) *J. Phys. Chem. Ref. Data* **1976**, *5*, 1129.

(13) Lossing, F. P. *J. Am. Chem. Soc.* **1977**, *99*, 7526.

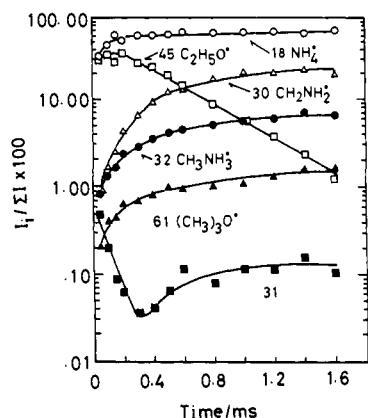


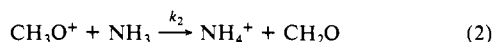
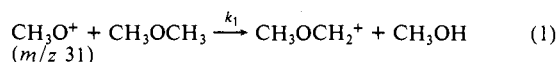
**Figure 1.** Normalized ion intensities vs. reaction time observed in the  $\text{CH}_3\text{OCH}_3\text{-NH}_3$  system.  $[\text{CH}_3\text{OCH}_3]/[\text{NH}_3] = 0.36$ , total ion source concentration =  $1.26 \times 10^{13}$  molecule/ $\text{cm}^3$ , ion source temperature = 433 K, and electron energy = 20 eV.

0.15 ms would be attributed to  $\text{H}^-$  abstraction reactions of ions  $\text{NH}_2^+$ ,  $\text{CH}_3^+$ , and  $\text{CH}_3\text{O}^+$  with  $\text{CH}_3\text{OCH}_3$ . There are three stable isomers of the  $\text{C}_2\text{H}_5\text{O}^+$  ion. They are methoxymethyl cation  $\text{CH}_3\text{OCH}_2^+$ , protonated ethylene oxide  $\text{CH}_2\text{-CH}_2$ , and protonated acetaldehyde  $\text{CH}_3\text{CHOH}^+$ . Three species have been identified experimentally.<sup>14</sup> It has been shown in several works<sup>2-6,13</sup> that the  $\text{C}_2\text{H}_5\text{O}^+$  ion derived from  $\text{CH}_3\text{OCH}_3$  by electron impact and the  $\text{H}^-$  abstraction reaction is the methoxymethyl cation. The experimental<sup>15</sup> and theoretical studies<sup>16</sup> of the  $\text{C}_2\text{H}_5\text{O}^+$  potential energy surface have shown that the isomerization

from  $\text{CH}_3\text{OCH}_2^+$  to  $\text{CH}_3\text{CHOH}^+$  ion proceeds through  $\text{CH}_2\text{-CH}_2$  as an intermediate. However, the process of the isomerization from

$\text{CH}_3\text{OCH}_2^+$  to  $\text{CH}_2\text{-CH}_2$  ion may have a very high barrier estimated to be  $\Delta H^\ddagger = \sim 97$  kcal/mol<sup>15</sup> or 89.7 kcal/mol.<sup>16</sup> These facts support that the ion involved in this study is mainly  $\text{CH}_3\text{OCH}_2^+$ , although the  $\text{CH}_3\text{OCH}_2^+$  ion would have various internal energies.

An initial decrease of  $\text{CH}_3\text{O}^+$  (time =  $\sim 0.3$  ms) in Figure 1 would be due to the reactions with  $\text{CH}_3\text{OCH}_3$  and  $\text{NH}_3$  shown in reactions 1 and 2. The rate constants measured are presented in Table I. The



increase of  $m/z \ 31$  at a longer ( $>0.3$  ms) reaction time is shown in the figure. Two ions,  $\text{CH}_2\text{OH}^+$  and  $\text{CH}_3\text{NH}_2^+$ , formed by the reaction between  $\text{CH}_3\text{OCH}_2^+$  and  $\text{NH}_3$  are conceivable.  $\text{CH}_2\text{OH}^+$  may be ruled out due to the subsequent rapid reaction with  $\text{NH}_3$  [ $k_{\text{ADO}}(\text{CH}_2\text{OH}^+ + \text{NH}_3) = 1.60 \times 10^{-9}$  cm<sup>3</sup>/(molecule·s) at 433 K].  $\text{CH}_3\text{NH}_2^+$  appears to be most likely. But the ion species  $m/z \ 31$  was not clearly identified, because the relative ion intensity was very small. The rate constants for the reactions of  $\text{CH}_3\text{O}^+$  with  $\text{CH}_3\text{OCH}_3$  and  $\text{NH}_3$  are in agreement with that obtained by Harrison<sup>2</sup> and that determined in our previous study,<sup>5</sup> respectively.

The ion species of  $m/z \ 30$  and  $32$  in Figure 1 were assigned to be  $\text{CH}_2\text{NH}_2^+$  and  $\text{CH}_3\text{NH}_3^+$  by using  $\text{ND}_3$  instead of  $\text{NH}_3$ . This result is in agreement with that reported by Kinter and Bursey.<sup>7</sup> The sum of relative ion intensities of  $\text{CH}_2\text{ND}_2^+$  and  $\text{CH}_3\text{ND}_3^+$  in  $m/z \ 30\text{-}35$  obtained in the  $\text{CH}_3\text{OCH}_3\text{-ND}_3$  system was  $\sim 94\%$ . This result shows that the H and D in the intermediate complex formed by the ion/molecule reaction of  $\text{CH}_3\text{OCH}_2^+$  with  $\text{NH}_3$  hardly scramble. Although there are two structural isomers,<sup>17-19</sup>  $\text{CH}_3\text{NH}^+$  and  $\text{CH}_2\text{NH}_2^+$ , as the  $m/z \ 30$  ion, the formation of  $\text{CH}_3\text{NH}^+$  is excluded. This is because the enthalpy

(14) Van de Graaf, B.; Dymerski, P. P.; McLafferty, F. W. *J. Chem. Soc., Chem. Commun.* **1975**, 978.

(15) Bowen, R. D.; Williams, D. H.; Hvistendahl, G. *J. Am. Chem. Soc.* **1977**, *99*, 7509.

(16) Nobes, R. H.; Rodwell, W. R.; Bouma, W. J.; Radom, L. *J. Am. Chem. Soc.* **1981**, *103*, 1913.

(17) Huntress, W. T., Jr.; Elleman, D. D. *J. Am. Chem. Soc.* **1970**, *92*, 3565.

(18) Lossing, F. P.; Lam, Y.-T.; Maccoll, A. *Can. J. Chem.* **1981**, *59*, 2228.

(19) Collin, J. E.; Franklin, M. J. *Bull. Soc. R. Sci. Liege* **1966**, *35*, 267.

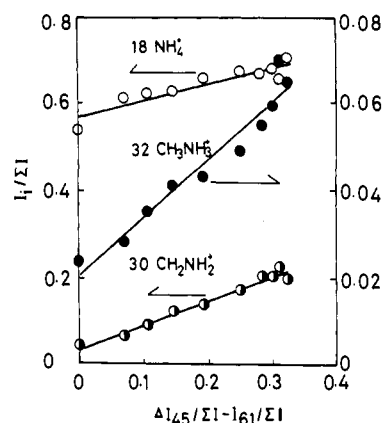
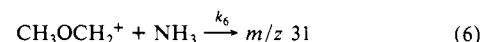
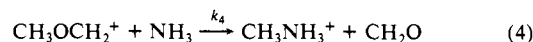
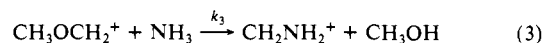
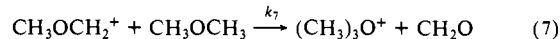


**Figure 2.** Normalized ion intensities vs.  $\Delta I_{45} - I_{61}$ . The same experimental conditions as in Figure 1 are used.

change of reaction for the formation of this ion is endothermic ( $\Delta H_f = 12.96$  kcal/mol). The reactions of  $\text{CH}_3\text{OCH}_2^+$  with  $\text{NH}_3$  at a longer time than 0.2 ms can be described by reactions 3-6.



In Figure 1, the  $m/z \ 61$  ion was observed at the same time scale. This ion is known to be  $(\text{CH}_3)_3\text{O}^+$ , formed by the ion/molecule reaction of  $\text{CH}_3\text{OCH}_2^+$  with  $\text{CH}_3\text{OCH}_3$  in only the dimethyl ether system,<sup>2</sup> as is given by reaction 7. The disappearance rate constant of  $\text{CH}_3\text{OCH}_2^+$



obtained was  $(1.4 \pm 0.6) \times 10^{-11}$  cm<sup>3</sup>/(molecule·s), which is in agreement with  $(1.16 \pm 0.15) \times 10^{-11}$  cm<sup>3</sup>/(molecule·s) reported by Harrison.<sup>2</sup>

The overall disappearance rate constant of  $\text{CH}_3\text{OCH}_2^+$  may be expressed by eq 8 in consideration of reactions 3-7.  $I_{45}$  is the normalized ion intensity of  $\text{C}_2\text{H}_5\text{O}^+$  ( $m/z \ 45$ ).  $[\text{NH}_3]$  and  $[\text{CH}_3\text{OCH}_3]$  are the concentrations of reactant molecules,  $t$  is the reaction time, and  $C$  is a constant.

$$\log I_{45} = -\left(\sum_{j=3}^6 k_j[\text{NH}_3] + k_7[\text{CH}_3\text{OCH}_3]\right)t + C \quad (8)$$

Each rate constant,  $k_i$ , was determined from the  $\Delta I$  plot<sup>20</sup> by using eq 9, where  $I_{si}$  is the normalized intensity of the secondary ion  $s_i$ ,  $k_i$  is the rate constant leading to the disappearance of  $\text{CH}_3\text{OCH}_2^+$ , and  $\sum_{j=3}^6 k_j$  is the rate constant for the reaction of  $\text{CH}_3\text{OCH}_2^+$  with  $\text{NH}_3$ .  $\Delta I_{45} =$

$$I_{si} = \frac{k_i}{\sum_{j=3}^6 k_j} (\Delta I_{45} - I_{61}) \quad (9)$$

$I_{45}^0 - I_{45}$ , where  $I_{45}^0$  is the normalized intensity of  $I_{45}$  extrapolated to reaction time, 0.2 ms.  $I_{61}$  is the normalized ion intensity of  $(\text{CH}_3)_3\text{O}^+$  ( $m/z \ 61$ ). The linear portion of a semilogarithmic plot for  $\text{CH}_3\text{OCH}_2^+$  gives the overall rate constant for the reaction of  $\text{CH}_3\text{OCH}_2^+$  with  $\text{NH}_3$  and  $\text{CH}_3\text{OCH}_3$ . The rate constant,  $\sum_{j=3}^6 k_j$ , was determined to be  $(2.30 \pm 0.1) \times 10^{-10}$  cm<sup>3</sup>/(molecule·s) by the use of eq 8, as the rate constant,  $k_7$ , was previously measured in only the  $\text{CH}_3\text{OCH}_3$  system.

Figure 2 shows a plot of  $I_{18}(\text{NH}_4^+)$ ,  $I_{32}(\text{CH}_3\text{NH}_3^+)$ , and  $I_{30}(\text{CH}_2\text{NH}_2^+)$  as a function of  $\Delta I_{45} - I_{61}$ . The straight lines are observed. The average slopes of five runs which give  $k_i/\sum_{j=3}^6 k_j$  were  $0.58 \pm 0.07$ ,  $0.16 \pm 0.02$ ,  $0.25 \pm 0.08$ , and  $\sim 0.004$ , respectively. These data for  $k_3$ ,  $k_4$ ,  $k_5$ , and  $k_6$  were obtained independently over the electron energy between 15 and 25 eV (not corrected).

More recent results<sup>7</sup> have indicated that the relative intensities of ions formed in reactions 3 and 4 decrease with increasing ion kinetic energy

(20) Myher, J. J.; Harrison, A. G. *J. Phys. Chem.* **1968**, *72*, 1905.

(21) *J. Phys. Chem. Ref. Data* **1977**, *6*, 1-776, 1-777.

(22) *J. Phys. Chem. Ref. Data* **1984**, *13*, 703, 709.

## Reactants

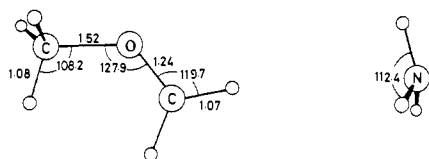


Figure 3. Geometries of methoxymethyl cation ( $C_2H_5O^+$ ) and ammonia optimized with the 3-21G basis set. Bond lengths are in Å and the angles are in deg. Empty small circles denote hydrogen atoms.

Table II. Rate Constants and Enthalpy Changes for the Reactions of  $CH_3OCH_2^+$  with  $NH_3$

reaction	$10^{-10}k_i, \text{cm}^3/(\text{molecule}\cdot\text{s})$		$\Delta H_r^a, \text{kcal/mol}$
	exptl	calcd ADO <sup>b</sup>	
$CH_3OCH_2^+ + NH_3 \xrightarrow{k_3}$ $CH_2NH_2^+ + CH_3OH$	$1.3_3 \pm 0.2$	16.8	$-16 (-20)^c$
$CH_3OCH_2^+ + NH_3 \xrightarrow{k_4}$ $CH_3NH_3^+ + CH_2O$	$0.37 \pm 0.05$		$-28 \pm 3^d$
$CH_3OCH_2^+ + NH_3 \xrightarrow{k_5}$ $CH_3CHO + CH_2^+$	$0.5_8 \pm 0.2$		
$NH_4^+ + \overline{O}-CH_2-CH_2$ ( $CH_3CHO$ ) <sup>e</sup>			$-8 \pm 3^d$
$CH_3OCH_2^+ + NH_3 \xrightarrow{k_6}$ $m/z\ 31$	$\sim 0.01$		$-35 \pm 3^d$

<sup>a</sup>  $\Delta H_f^{298}(CH_3OCH_2^+) = 157 \text{ kcal/mol}$  from ref 13.  $\Delta H_f^{298}(CH_2NH_2^+) = 178$  and  $174 \text{ kcal/mol}$  from ref 18 and 19.  $\Delta H_f^{298}(CH_3NH_3^+) = 146 \text{ kcal/mol}$  is calculated by using  $\Delta H_f^{298}(CH_3NH_2) = -5.49 \text{ kcal/mol}$  from ref 21.  $\Delta H_f^{298}(H^+) = 367.7 \text{ kcal/mol}$  is taken from ref 22.  $PA(CH_3NH_2) = 214.1 \text{ kcal/mol}$  is taken from ref 22.  $\Delta H_f^{298}(NH_4^+) = 150.68 \text{ kcal/mol}$  is calculated by using  $\Delta H_f^{298}(NH_3) = -11.02 \text{ kcal/mol}$  from ref 21.  $PA(NH_3) = 204 \text{ kcal/mol}$  is taken from ref 22.  $\Delta H_f^{298}(CH_3OH) = -47.96 \text{ kcal/mol}$ ,  $\Delta H_f^{298}(CH_2O) = -28 \text{ kcal/mol}$ ,  $\Delta H_f^{298}(\overline{O}-CH_2-CH_2) = -12.58 \text{ kcal/mol}$ , and  $\Delta H_f^{298}(CH_3CHO) = -39.72 \text{ kcal/mol}$  are from ref 21. <sup>b</sup> Calculated by using the ADO theory.<sup>23</sup> <sup>c</sup>  $\Delta H_f^{298}(CH_2NH_2^+) = 174 \text{ kcal/mol}$  is used.<sup>19</sup> <sup>d</sup> Deviation was that of  $PA(NH_3)$ .<sup>22</sup> <sup>e</sup> The  $\Delta H_r$  value for this product is  $-35 \pm 3^d \text{ kcal/mol}$ .

and that reaction 5 has the threshold energy,  $\Delta H_r = 55.32 \text{ kcal/mol}$  (center of mass). It has been pointed out<sup>7</sup> that reaction 5 is not expected at low ion kinetic energies. As electron energies  $\geq 15 \text{ eV}$  were used in this study to generate  $CH_3OCH_2^+$  from  $CH_3OCH_3$ , reaction 5 can be observed. Therefore, the  $CH_3OCH_2^+$  ions formed would have enough of the internal energies<sup>3</sup> needed for reaction 5.

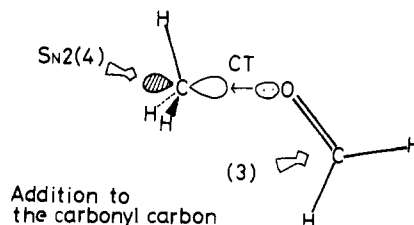
The individual rate constants and enthalpy changes for the reaction of  $CH_3OCH_2^+$  with  $NH_3$  are obtained and are presented in Table II. The collision rate constant calculated by average dipole orientation (ADO) theory<sup>23</sup> is also shown in Table II.

## Computations

To identify the product and to elucidate the route of reactions between methoxymethyl cation and ammonia, reactions 3, 4, and 5, an ab initio MO calculation is made. The geometries of reactants, ion-dipole complexes, and transition states are searched for by the optimization with the 3-21G basis set. Energies and electronic distributions are obtained by the single-point calculation of 6-31G\* (6-31G\*\*//3-21G). All calculations are carried out using the GAUSSIAN 80 program.<sup>24</sup>

In Figure 3, geometries of  $C_2H_5O^+$  and  $NH_3$  are shown. Theoretical studies of methoxymethyl cation have been made extensively.<sup>16,25</sup> However, the structural picture is not clear yet. The most stable isomer of  $C_2H_5O^+$  is regarded as a Mulliken charge-transfer (CT) complex between formaldehyde and methyl

cation. In the picture below, two reactive sites for the nucleophile may be indicated by bold empty arrows.

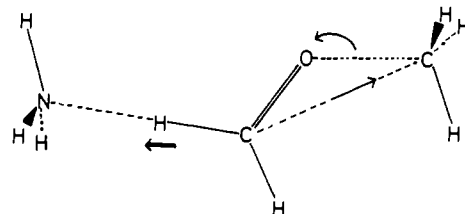


When the carbonyl carbon of formaldehyde is attacked by  $NH_3$ , reaction 3 takes place. In Figure 4, the reaction process is exhibited. When  $NH_3$  collides with  $C_2H_5O^+$ , a stable intermediate called the ion-dipole complex I is formed. It is another strong ( $\rightarrow N \rightarrow >C \equiv$ ) CT complex. After the complex is generated, the reaction proceeds by the ammonia-proton migration. In the transition state, bridge  $O \cdots H$  and  $H \cdots N$  bonds are found. The more electronegative oxygen atom pulls the proton away from the nitrogen atom. Then, the second stable intermediate II is generated, followed by product formation (methanol and protonated methylenimine). Reaction 3 is composed of the nucleophilic addition onto the unsaturated carbon and the subsequent proton migration between two heteroatoms.

When the back side of the methyl cation of methoxymethyl cation is attacked by  $NH_3$ , the  $S_N2$ -type reaction 4 occurs. In Figure 5, the reaction process is exhibited. First,  $NH_3$  is captured by the methyl hydrogen to form the intermediate I. Second, at the transition state (TS), the bond interchange ( $N \cdots C-O \rightarrow N-C \cdots O$ ) and the Walden inversion take place. Third, the intermediate II is formed. Products are formaldehyde (leaving group of  $S_N2$ ) and protonated methylamine.

The reaction patterns of 3 and 4 are readily predictable in terms of the shape of the methoxymethyl cation,  $CH_3^+ \cdots O=CH_2$ . In contrast, it is somewhat difficult to say what kind of reaction mechanism is involved in reaction 5. To give  $NH_4^+$  as a product, a proton should be removed from  $CH_3^+ \cdots O=CH_2$ . To diminish the large destabilization caused by the scission of the tight C-H  $\sigma$  bond, a new bond formation is required. According to this criterion, the reaction path of reaction 5 is sought. The result is shown in Figure 6. The intermediate I is common to that of reaction 4. At TS, the proton shift and the C-C bond formation (ring closure) occur concertedly. After the intermediate II is generated, products (ammonium ion and ethylene oxide) are given. Thus, the ethylene oxide formation is found by the calculation.

As an alternative product, acetaldehyde is considered. The enthalpy changes for the formation of ethylene oxide and acetaldehyde are  $-8 \pm 3$  and  $-35 \pm 3 \text{ kcal/mol}$ , respectively. Since the  $CH_3CHO$  formation is more exothermic, the route to it appears to be more likely than to ethylene oxide as reaction 5. However, by the potential energy search, we cannot find any reasonable path leading to  $CH_3CHO$ . The C-H bond of formaldehyde is too tight



to break. Although the reaction (reaction 5) for the ethylene oxide is unfamiliar, the reverse reaction is the standard organic chemical reaction. The reverse reaction gives the electrophilic ring cleavage of the epoxide, where the similar ring opening of the cyclopropane derivatives is well-known.

Total energies ( $E_T$ 's) of species appearing in Figures 3, 4, 5, and 6 are computed with the 6-31G\* basis set and are shown in Table III. The theoretical enthalpy change  $\Delta H_r$  is approximately given by the difference of  $E_T$ 's between reactants and products.<sup>26</sup>

(23) Su, T.; Bowers, M. T. *Int. J. Mass Spectrom. Ion Phys.* **1973**, *12*, 347.

(24) Binkley, J. S.; Whiteside, R. A.; Krishnan, R.; Seeger, R.; DeFrees, D. J.; Schlegel, H. B.; Topiol, S.; Kahn, L. R.; Pople, J. A. *QCPE* **1981**, *13*, 406.

(25) Fărcașiu, D.; Horsley, J. A. *J. Am. Chem. Soc.* **1980**, *102*, 4906.

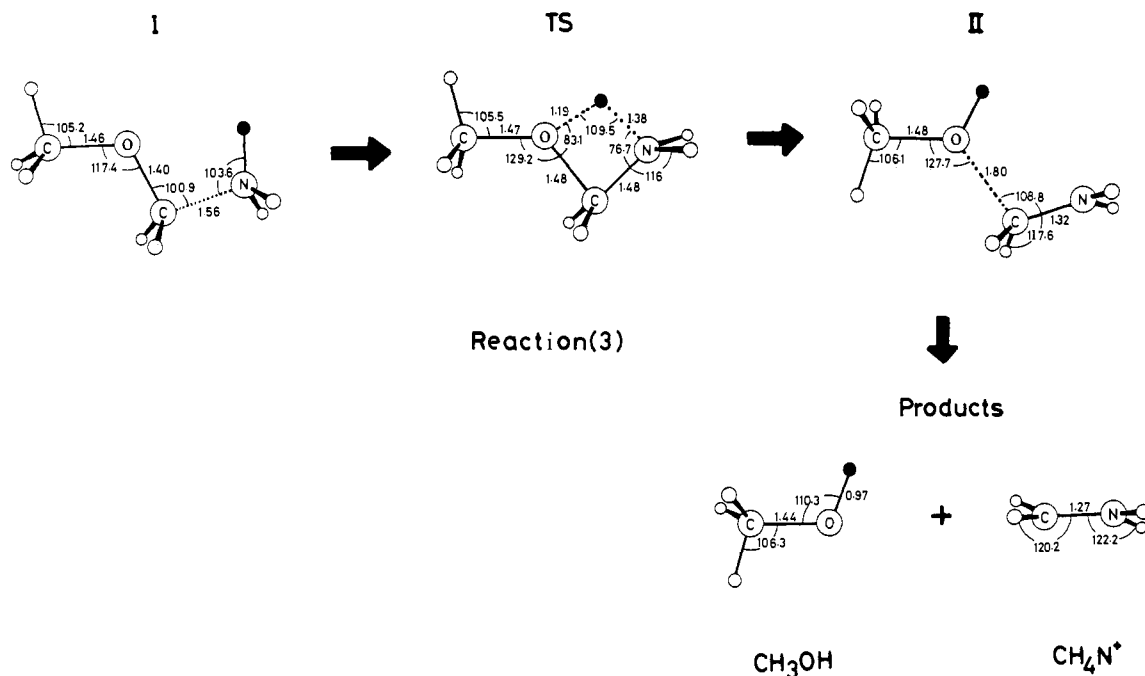


**Figure 4.** Geometries of two ion-dipole complexes (I and II), the transition state (TS), and the product in reaction 3. A black circle is the proton to be migrated.

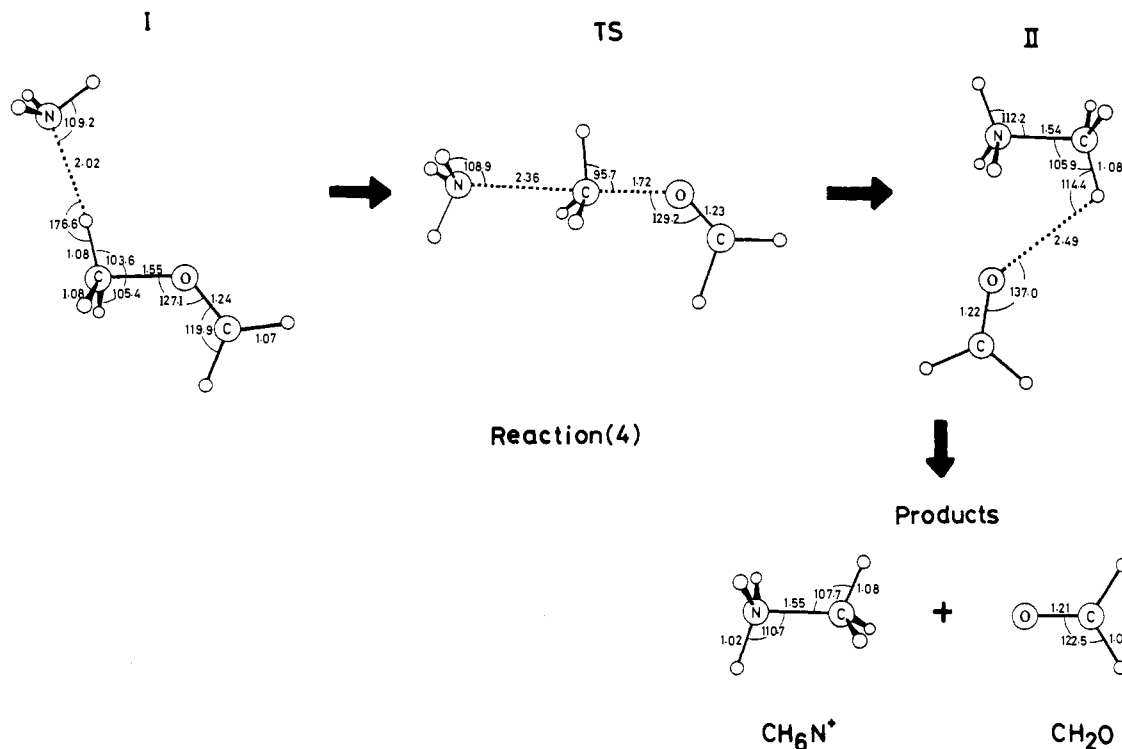


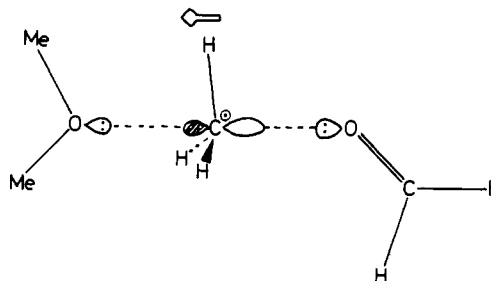
**Figure 5.** Geometries of two ion-dipole complexes (I and II), the transition state (TS), and the product in reaction 4.

Calculated and estimated (exptl)  $\Delta H_f$ 's of reactions 3 and 4 are in good agreement, but those of reaction 5 are somewhat different. One reason for this discrepancy lies in the choice of the heat of formation.

In Figure 7,  $E_T$ 's are displayed. Three curves of reactions 3, 4, and 5 show the typical Braumann's double-well potential. The intermediate I of reaction 3 gets the large ( $-40.83$  kcal/mol) stability due to CT. The large activation energy barrier of reaction 5 is also noticeable, which is needed for the C-H bond cleavage.

Reaction 7 is composed of the methyl cation shift between two bases (formaldehyde and dimethyl ether). The migration is a

ready process, as is understandable by the difference of the proton affinities,  $\text{PA}(\text{CH}_2\text{O}) = 171.7$  vs.  $\text{PA}(\text{CH}_3\text{OCH}_3) = 192.1$  kcal/mol.<sup>22</sup>



(26) The difference of theoretical  $\Delta E_T$  and theoretical  $\Delta H_f$  is known to be small ( $\sim 1$  or 2 kcal/mol).

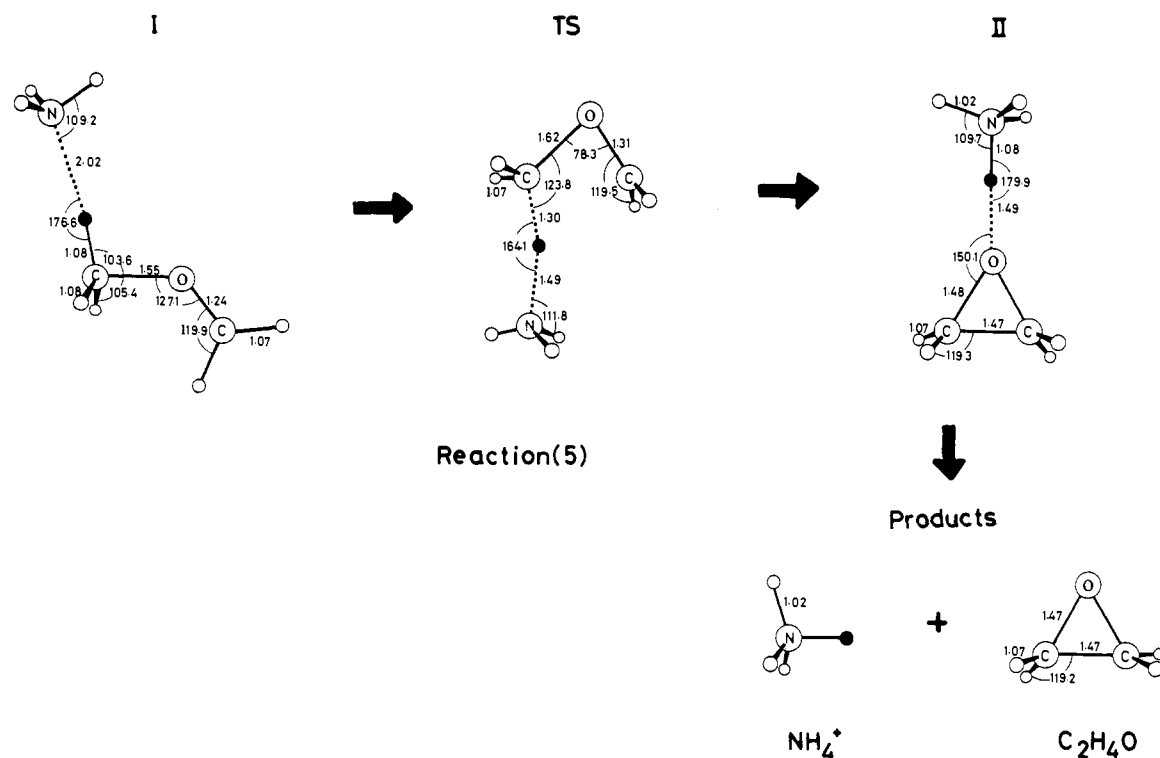


**Figure 6.** Geometries of two ion-dipole complexes (I and II), the transition state (TS), and the product in reaction 5. The small black circle denotes the proton to be migrated.

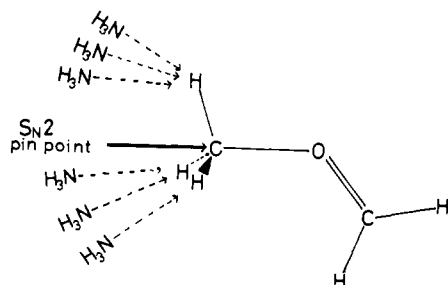
**Table III.** Total Energies ( $E_T$ 's) and Exothermicities ( $\Delta H_r$ 's) of Reactions 3, 4, and 5<sup>a</sup>

reactants	reaction	$E_T$ , hartree			products	$\Delta H_r$ , kcal/mol	
		ion-dipole complex I	TS	ion-dipole complex II		calcd	exptl <sup>b</sup>
NH <sub>3</sub> , -56.182 499	3	-209.449 207	-209.386 494	-209.429 923	CH <sub>3</sub> OH, -115.033 753	-20.50	-16 (-20) <sup>c</sup>
	4	-209.400 017	-209.395 498	-209.464 232	CH <sub>4</sub> N <sup>+</sup> , -94.383 056	-33.73	-28 ± 3 <sup>d</sup>
					CH <sub>2</sub> O, -113.865 299		
					CH <sub>6</sub> N <sup>+</sup> , -95.572 598		
C <sub>2</sub> H <sub>3</sub> O <sup>+</sup> , -153.201 642	5	-209.400 017	-209.321 097	-209.428 131	CH <sub>2</sub> -CH <sub>2</sub> , -152.861 878	-5.20	-8 ± 3 <sup>d</sup>
					CH <sub>3</sub> CHO, -152.913 362	-37.52	-35 ± 3 <sup>d</sup>
					CH <sub>2</sub> CHOH, -152.884 013	-19.10	
					NH <sub>4</sub> <sup>+</sup> , -56.530 551		

<sup>a</sup> 1 hartree = 627.566 kcal/mol. <sup>b</sup> Experimental data are those shown in Table II. <sup>c</sup>  $\Delta H_f^{298}(CH_2NH_2^+) = 174$  kcal/mol<sup>19</sup> is used. <sup>d</sup> Deviation was that of PA(NH<sub>3</sub>).<sup>22</sup>

## Discussion

Reactions 3, 4, and 5 are examined kinetically and theoretically. Rate constants in Table II are in the order  $k_3 > k_5 > k_4$ . In view of the potential energy profiles in Figure 7, it seems strange that reaction 5 is faster than reaction 4. Two reactions have the common intermediate I. It is noteworthy that the gas-phase reaction has a peculiar reactivity, when the methyl hydrogen is attacked by a nucleophile. The reaction channel of reaction 4, i.e., S<sub>N</sub>2, is sterically quite narrow. The S<sub>N</sub>2 path is just a



pinpoint. If the approaching NH<sub>3</sub> misses it, only the elastic collision takes place. The isomerization of the intermediate I to

the net S<sub>N</sub>2 is not so likely under the present large internal energy (the electron energies of  $\geq 15$  eV were used to generate CH<sub>3</sub>OCH<sub>2</sub><sup>+</sup> from CH<sub>3</sub>OCH<sub>3</sub>). Thus, the pinpoint penetration is of a small probability, leading to the small Arrhenius factor in spite of the low activation barrier. Reactions 3 and 5 do not suffer from the block of the methyl hydrogens.

Kinter and Bursley<sup>7</sup> have studied the same ion/molecule reaction with the triple-quadrupole instrument where the kinetic analysis has not been made. Their spectral data, translational energy vs. ion yields, may be discussed in terms of the present result. The ion intensity of CH<sub>2</sub>NH<sub>2</sub><sup>+</sup> produced by reaction 3 is not so affected by the magnitude of the ion kinetic energy (1.5–7 eV).<sup>7</sup> The deep potential well of the intermediate I is thought to hold a probability of the nonelastic collision effectively. Next, the intensity of the product ion NH<sub>4</sub><sup>+</sup> is reported<sup>7</sup> to increase monotonically as the ion kinetic energy is enlarged, with the threshold value = 55 ± 5 kcal/mol. This energy is somewhat larger than our activation barrier, 39.56 kcal/mol, of reaction 5. Interestingly, the energy of 55 ± 5 kcal/mol is found to be almost the same as our barrier, 49.52 kcal/mol (=39.56 + 9.56 kcal/mol), relative to the energy of the intermediate I. Therefore, the product (ethylene oxide, not ·CH<sub>2</sub>-O-CH<sub>2</sub>· which they assumed) of the exothermic reaction 5 is confirmed by this agreement. The ion intensity of CH<sub>3</sub>NH<sub>3</sub><sup>+</sup> of reaction 4 is decayed as the kinetic energy increases.<sup>7</sup> Reactions

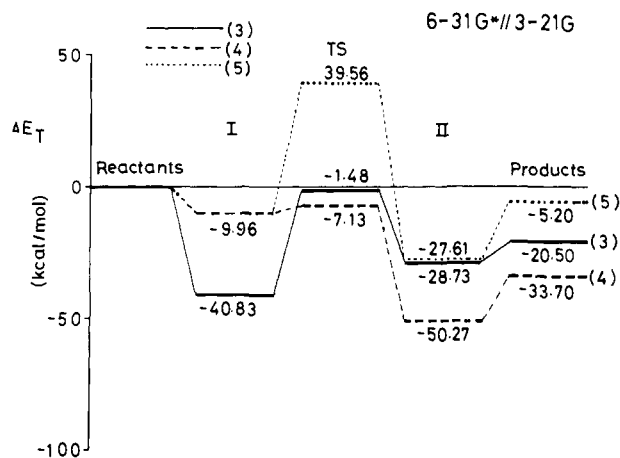


**Figure 7.** Potential energy profiles of reactions 3, 4, and 5. I and II denote ion-dipole complexes, and TS means the transition state. Energies in the figure stand for the stabilizing (<0) or destabilizing (>0) values relative to those of reactants.

4 and 5 are competitive, holding the intermediate I in common. By the larger kinetic energy, reaction 4 becomes minor as reaction 5 with the larger activation barrier becomes dominant. The large kinetic energy gives either the simple elastic collision (no  $S_N2$ ) between the methyl hydrogen of  $CH_3OCH_2^+$  and  $NH_3$  or reaction 5.

### Concluding Remarks

In this work, the kinetics of the three gas-phase reactions, reactions 3, 4, and 5, between methoxymethyl cation and ammonia has been determined at 433 K. The result in Table II shows the similar rate constants where the rank is  $k_3 > k_5 > k_4$ . An ab initio MO calculation has given the potential energy profile of the three reactions. Reaction 3 consists of the nucleophilic attack of  $NH_3$  to the carbonyl carbon and the 1,3-proton shift from the nitrogen to the oxygen atom. The kinetic efficiency of reaction 3 is ascribed to the substantial stability of the intermediate I (i.e., the long-lived collision complex). Reaction 4 is of the  $S_N2$  type and is not efficient due to the short-lived intermediate I and the pinpoint target of the back-side attack. Reaction 5 is composed of the concerted motion of the proton shift and the ring closure. Although reaction 5 has a large activation barrier, it is more efficient than reaction 4 through the effective conversion<sup>7</sup> of the translation energy to the internal energy and the absence of the methyl hydrogen block.

Reactions 3 and 4 involve the representative mechanisms of organic chemistry. Reaction 5 is a characteristic gas-phase process under the abundant translation energy. The methyl hydrogen may be hardly abstracted in the mild conditions of the aqueous media.

**Acknowledgment.** We thank the Data Processing Center of Kyoto University for the allotment of the CPU time of the FACOM M-382 computer. Thanks are also due to the Institute for Molecular Science for our use of the HITAC M-200H computer.

**Registry No.**  $MeOCH_2^+$ , 23653-97-6;  $NH_3$ , 7664-41-7.

## Infrared Spectra of Alkali Metal Atom-Ammonia Complexes in Solid Argon

Sefik Süzer and Lester Andrews\*

Contribution from the Chemistry Department, University of Virginia, Charlottesville, Virginia 22901, and Middle East Technical University, Ankara, Turkey.  
Received June 2, 1986

**Abstract:** One-to-one complexes between Li, Na, K, and Cs atoms and  $NH_3$  have been studied by using matrix IR spectroscopy. New bands at 1133, 1079, 1064, and 1049  $cm^{-1}$  are assigned to perturbed  $\nu_2$  modes, and bands at 3277, 3294, 3292, and 3287  $cm^{-1}$  are assigned to the perturbed  $\nu_1$  ammonia submolecule modes of the Li- $NH_3$ , Na- $NH_3$ , K- $NH_3$ , and Cs- $NH_3$  complexes, respectively. The corresponding bands for K and  $^{15}NH_3$ ,  $NH_2D$ ,  $NHD_2$ , and  $ND_3$  complexes are also assigned. The intensity ratios of  $\nu_1$  to  $\nu_2$  for the ammonia submolecule modes in the Li, Na, K, and Cs complexes are larger by factors of 15, 20, 30, and 35, respectively, than the corresponding ratio for isolated ammonia. The intensification and position of  $\nu_1$  in the complex and the alkali metal-ammonia interaction are consistent with calculations of a very small ammonia  $\rightarrow$  metal charge transfer where the alkali atom acts as a weak Lewis acid for Li and Na. The increased ammonia interaction with K and Cs may suggest a possible acid-base role reversal for the heavier alkali complexes. At higher metal/ammonia concentrations higher aggregate bands of  $(M)_n-NH_3$  nature are also observed.

Solutions of alkali metal in liquid ammonia have been the subject of numerous studies dating back more than a century.<sup>1-3</sup> The well-known reactions of alkali metals with liquid water and ammonia are highly exothermic, and solvation of the alkali cation and electron formed provide major contributions to the exothermicity of the reaction. At the molecular level in the gas phase, however, the reactivity is expected to be greatly reduced. Ab initio SCF calculations<sup>4,5</sup> predict a 14.5 kcal/mol binding energy for

Li- $NH_3$  but only 6.0 kcal/mol for Na- $NH_3$ , as compared to 33 and 29 kcal/mol, respectively, for the corresponding ion-molecule complexes  $Li^+-NH_3$  and  $Na^+-NH_3$  observed by high-pressure mass spectrometry in the gas phase.<sup>6</sup> No calculations exist for larger alkali atom complexes, but experimentally measured binding energies decrease steadily going down the series for the cation-ammonia complexes. The ESR spectrum of the Li- $NH_3$  complex in solid argon indicates a reduced spin density localized in the lithium 2s orbital.<sup>7</sup> Although chemical intuition

(1) *Colloque Weyl I: Metal-Ammonia Solutions*; Lepoutre, G., Sienko, M., Eds.; Benjamin: New York, 1964.

(2) *Colloque Weyl II: Metal-Ammonia Solutions*; Lagowski, T., Sienko, M., Eds.; Butterworths: London, 1970.

(3) Jolly, W. L. *Metal-Ammonia Solutions*; Dowden, Hutchinson, and Ross: Stroudsburg, PA, 1972.

(4) Nicely, V. A.; Dye, J. L. *J. Chem. Phys.* **1970**, *52*, 4795.

(5) Trenary, M.; Schaefer, H. F., III; Kollman, P. *J. Am. Chem. Soc.* **1977**, *99*, 3885.

(6) Castleman, A. W., Jr.; Holland, P. M.; Lindsay, D. M.; Peterson, K. *J. Am. Chem. Soc.* **1978**, *100*, 6039.

(7) Meier, P. F.; Hauge, R. H.; Margrave, J. L. *J. Am. Chem. Soc.* **1978**, *100*, 2108.